Journal of Applied Analysis and Computation
Volume 9, Number 6, December 2019, 2261–2277
Website:http://jaac.ijournal.cn
DOI:10.11948/20190032

GEOMETRICAL ANALYSIS OF A PEST MANAGEMENT MODEL IN FOOD-LIMITED ENVIRONMENTS WITH NONLINEAR IMPULSIVE STATE FEEDBACK CONTROL*

Tongqian Zhang[1,2,†], Tong Xu[1], Junling Wang[1], Yi Song[1] and Zhichao Jiang[3]

Abstract In this paper, a nonlinear impulsive state feedback control system is proposed to model an integrated pest management in food-limited environments. In the system, impulsive feedback control measures are implemented to control pests on the basis of the quantitative state of pests. Mathematically, an intuitive geometric analysis is used to indicate the existence of periodic solutions. The stability of periodic solutions is investigated by using Analogue of Poincaré Criterion. At last, numerical simulations are given to verify the theoretical analysis.

Keywords Integrated Pest Management (IPM), impulsive state feedback control, limited food environment, periodic solutions, stability.

MSC(2010) 34C25, 34C60, 92B05.

1. Introduction and model formulation

Agricultural pests have always threatened agricultural production, and large-scale pests may even cause crop outbreaks. Farmers and agricultural scientists have been looking for an effective way to control pests. The advent of chemical pesticides and their wide range of using effectively solved the problem of insect pests in a short

† the corresponding author. Email address:zhangtongqian@sdust.edu.cn (T. Zhang)

[1] College of Mathematics and Systems Science, Shandong University of Science and Technology, Qingdao 266590, China

[2] State Key Laboratory of Mining Disaster Prevention and Control Co-founded by Shandong Province and the Ministry of Science and Technology, Shandong University of Science and Technology, Qingdao 266590, China

[3] Fundamental Science Department, North China Institute of Aerospace Engineering, Langfang 065000, China

* T. Zhang was supported by Shandong Provincial Natural Science Foundation of China (No. ZR2019MA003), SDUST Research Fund (No. 2014TDJH102) and Scientific Research Foundation of Shandong University of Science and Technology for Recruited Talents. T. Xu and J. Wang was supported by SDUST Innovation Fund for Graduate Students (No. SDKDYC190119). Z. Jiang was supported by National Natural Science Foundation of China (Nos. 11801014 and 11875001), Natural Science Foundation of Hebei Province (No. A2018409004), Hebei province university discipline top talent selection and training program (SLRC2019020) and Talent Training Project of Hebei Province.

period of time. However, the evidence shows that with the abuse of pesticides, many problems have begun to emerge, such as the contamination of water and soil caused by the residues of pesticides, the resistance of pests, etc [2,12,22,45].

Integrated Pest Management (IPM) is a comprehensive technique for controlling pests using chemical, physical, biological, agricultural and cultural methods [1,37]. The purpose of IPM is to control the number of pests within a certain range, instead of eradicating pests. Because it can control pests and protect the environment to the greatest extent, IPM has been welcomed and paid much attention by many researchers [20,27,32,35,39,43]. One commonly used chemical control method is spraying pesticides, another commonly used biological control method is releasing natural enemies that are cultivated in the laboratory. The implementation of artificial intervention measures will lead to rapid changes in the number of biological populations. This phenomenon can be characterized by impulsive differential equations [6,7,9,21,24,26,33,52,56]. To understand the evolutionary relationship between pests and natural enemies under artificial control strategies in IPM, based on the predator-prey model [15,16,30,31,49,57,58], Liu et al [23] proposed a two dimensional IPM model with pulses as follows,

$$\begin{cases} \left.\begin{aligned} {u_1}' &= u_1(r - au_1 - bu_2), \\ {u_2}' &= u_2(cu_1 - u_2), \end{aligned}\right\} t \neq nT, \\ \left.\begin{aligned} \Delta u_1 &= -p_1 u_1, \\ \Delta u_2 &= -p_2 u_2 + \tau, \end{aligned}\right\} t = nT, \end{cases} \tag{1.1}$$

where u_1 and u_2 represent the density or number of pests and natural enemies, respectively. Δu_i represent the variation of u_i and is defined as $u_i(t^+) - u_i(t), i = 1, 2$. p_1 and p_2 are kill rate of the pesticide for pests and natural enemies, respectively. τ represents the release amount of natural enemies for each impulsive period T.

However, in actual pest management, considering the cost, efficiency and operability, generally only the number of pests runs up to a certain threshold, and IPM is implemented to kill pests. In other words, we determine whether to implement integrated management based on the number or density of pests. This process can be described by a state feedback control system [4,18,25,29,44,46,48], because the state of the system variable has changed dramatically after each feedback control, this feedback control is also called impulsive state feedback control which has been extensively used to explain the implementation of control measures in population models [14,19,51,53], chemostat models [11,41,50], turbidostat models [47,55] and epidemic models [8,10,28,38,54].

In [40], Tang et al. constructed an IPM model as follows,

$$\begin{cases} \left.\begin{aligned} u_1' &= u_1(a - bu_2), \\ u_2' &= u_2(cu_1 - d), \end{aligned}\right\} u_1 \neq ET, \\ \left.\begin{aligned} \Delta u_1 &= -pu_1, \\ \Delta u_2 &= \tau, \end{aligned}\right\} x = ET, \end{cases} \tag{1.2}$$

the authors assumed that IPM is carried out to kill the pest once the number of pests reach a certain threshold ET. They proved that system (1.2) has one order one periodic solution by constructing Poincaré map. Zhang et al. [51] improved model (1.2) by adopting logistic growth for the pest population. However, in the process of investigating the population growth of Daphnia magna, Smith [36] founded that the hypothesis of linear average growth rate is not reasonable and proposed a food limited population growth model with the form

$$x'(t) = rx(t)\frac{K - x(t)}{K + \frac{r}{e}x(t)}. \tag{1.3}$$

In the model (1.3), food is mainly used to keep the survival and growth of the population. The model is proposed based on the assumption that the population is no longer growing when it reaches saturation, and in this case, food is only used to keep the survival of the population. Obviously, equation (1.2) is a generalized logistic equation.

Thus based on the hypothesis of [3, 36] and previous works [42, 51], we propose an impulsive state feedback control system to model an integrated pest management in limited food environment as follows,

$$\begin{cases} \left.\begin{array}{l} x' = rx\frac{K-x}{K+\frac{r}{e}x} - \beta xy, \\ y' = \lambda\beta xy - dy, \end{array}\right\} x \neq h, \\ \left.\begin{array}{l} \Delta x = -p(x)x, \\ \Delta y = -qy + \tau, \end{array}\right\} x = h, \end{cases}$$

where x and y represent the density or number of pests and natural enemies, respectively. $0 \le q < 1$ represents kill rate of the pesticide for natural enemies. $\tau \ge 0$ is the release amount of natural enemies. Because of the limited resources and the development of insect resistance to insecticides and other factors, insecticides have saturation effect on pests. To characterize this saturation effect of insecticides on the pests, the proportion of each killed pests p can be changed as a saturation function dependent pest populations, namely, $p(x(t)) = \frac{P_{\max}x(t)}{x(t)+\theta}$, and $P_{\max} \in [0, 1)$ is the maximal killing rate, θ is the half saturation constant [42]. The meaning of parameters r, K, e are same as equation (1.1). Detailed biological explanations of system (1.2), we refer to reference [23, 42, 51]. For the sake of simplicity, let $r = a$, $\frac{r}{K} = b$, $\frac{r}{Ke} = c$, we get the model as follows,

$$\begin{cases} \left.\begin{array}{l} x' = x\frac{a-bx}{1+cx} - \beta xy, \\ y' = \lambda\beta xy - dy, \end{array}\right\} x \neq h, \\ \left.\begin{array}{l} \Delta x = -p(x)x, \\ \Delta y = -qy + \tau, \end{array}\right\} x = h. \end{cases} \tag{1.4}$$

Considering the biological meaning, we will consider the solution of system (1.4) in region $R^2_+ = \{(x, y)|x \ge 0, y \ge 0\}$.

The organization of this paper is as follows. We qualitatively analyze the system (1.4) neglecting nonlinear pulsed effect in Sect. 2. And in Sect. 3, we consider the existence and stability of order one periodic solution of system (1.4). In Sect. 4, numerical simulations are carried out to illustrate the analytical results. We give a brief conclusion in Sect. 5.

2. Equilibria stability analysis of the system neglecting impulsive effect

Let $p_{\max}, q, \tau = 0$ in system (1.4), we obtain a system neglecting impulsive effect in the form of

$$\begin{cases} x' = x\frac{a-bx}{1+cx} - \beta xy, \\ y' = \lambda\beta xy - dy. \end{cases} \tag{2.1}$$

By solving

$$\begin{cases} x\frac{a-bx}{1+cx} - \beta xy = 0, \\ \lambda\beta xy - dy = 0, \end{cases} \tag{2.2}$$

we know that system (2.1) always have a trivial equilibrium $A(0,0)$ and a semi-trivial equilibrium $B(a/b,0)$, if and only if $(H_1) : \lambda\beta a > bd$ holds, system (2.1) also has a positive equilibrium $E(x^*, y^*)$, where $x^* = \frac{d}{\lambda\beta}, y^* = \frac{a-bx^*}{\beta(1+cx*)}$.

Let $(\overline{H_1}) : \lambda\beta a < bd$, the Jacobian of the equilibria has the following form

$$J = \begin{pmatrix} \frac{a-2bx-bcx^2}{(1+cx)^2} - \beta y & -\beta x \\ \lambda\beta y & \lambda\beta x - d \end{pmatrix}.$$

At $A(0,0)$, we have

$$J(A) = \begin{pmatrix} a & 0 \\ 0 & -d \end{pmatrix},$$

obviously, $A(0,0)$ is a saddle point. At $B(a/b,0)$, we have

$$J(A) = \begin{pmatrix} \frac{-ab}{ac+b} & -\beta\frac{a}{b} \\ 0 & \lambda\beta\frac{a}{b} - d \end{pmatrix},$$

obviously, if (H_1) holds, then $B(a/b,0)$ is a saddle point and if $\overline{H_1}$ holds, then $B(a/b,0)$ is a stable node.

And at $E(x^*, y^*)$, we get

$$J(E^*) = \begin{pmatrix} -\frac{(b+ac)x^*}{(1+cx^*)^2} & -\beta x^* \\ \lambda\beta y^* & 0 \end{pmatrix}.$$

Let $A = \frac{(b+ac)x^*}{(1+cx^*)^2}, B = \lambda\beta^2 x^* y^*$, the two eigenvalues λ_1, λ_2 of $J(E^*)$ satisfy

$$\lambda_1 + \lambda_2 = -A < 0,$$
$$\lambda_1\lambda_2 = B > 0.$$

Obviously, E^* is locally asymptotically stable. Moreover, let $\Delta = A^2 - 4B$, and when $\Delta < 0$, $E(x^*, y^*)$ is a stable focus.

Let $H_2 : \Delta < 0$, then we have the following theorem.

Theorem 2.1. *If (H_1) and (H_2) hold, then $E(x^*, y^*)$ is a stable focus.*

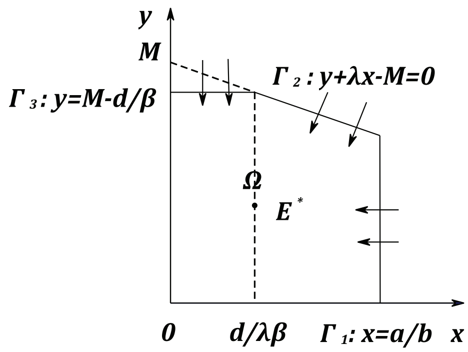

Figure 1. The solution of system (2.1) is bounded.

Theorem 2.2. *The solution of system* (2.1) *is ultimately bounded.*

Proof. Given the initial conditions

$$x(t_0) = x_0 > 0, y(t_0) = y_0 > 0. \tag{2.3}$$

Let $(x(t), y(t))$ be a solution of system (2.1) satisfied initial conditions (2.3). We will build a area Ω with a boundary such that $(x(t), y(t)) \in \Omega$ for initial point $(x(t_0), y(t_0))$ and $t > T$, where $T > 0$ is large (see Figure 1). Since point $B(a/b, 0)$ ia a saddle point, for line $\Gamma_1 : x - a/b = 0$ passing through B, we have

$$\frac{d\Gamma_1}{dt}\bigg|_{\Gamma_1=0} = x\frac{a-bx}{1+cx} - \beta xy\bigg|_{\Gamma_1=0} = -\beta\frac{a}{b}y < 0.$$

Thus the line Γ_1 is a segment without contact and orbit of system (2.2) goes across it from the right. On the other hand, define in the first quadrant:

$$\Gamma_2 : y + \lambda x - M = 0, \Gamma_3 : y - M + \frac{d}{\beta} = 0.$$

Then we have

$$\begin{aligned}
\frac{d\Gamma_2}{dt}|_{\Gamma_2=0} &= \left[y(\lambda\beta x - d) + \lambda x\left(\frac{a-bx}{1+cx} - \beta y\right)\right]\bigg|_{\Gamma_2=0} \\
&= \lambda x\left(\frac{a-bx}{1+cx} + d\right) - Md, \\
\frac{d\Gamma_3}{dt}|_{\Gamma_3=0} &= y(\lambda\beta x - d).
\end{aligned}$$

Thus, we have $d\Gamma_2/dt < 0$ for $d/\lambda\beta < x < a/b$ and $d\Gamma_3/dt < 0$ for $0 < x < d/\lambda\beta$, here M is large enough. So there exists a area Ω with a boundary being composed of $x = 0, y = 0, \Gamma_1\Gamma_2$ and Γ_3 such that $(x(t), y(t)) \in \Omega$ for initial point $(x(t_0), y(t_0))$ and $t > T$, where $T > 0$ is large. This completes the proof. $\square$

Theorem 2.3. *If* (H_1) *and* (H_2) *hold, then* $E(x^*, y^*)$ *is global asymptotically stable.*

Proof. Construct Dulac function $B = \frac{1}{xy}$, it is easy to check

$$D = \frac{\partial(PB)}{\partial x} + \frac{\partial(QB)}{\partial y} = -\frac{ac+b}{(1+cx)^2 y} < 0.$$

By the Bendixson-Dulac theorem [13], we have there is no closed orbit around E. Then by theorems 2.1 and 2.2, E is global asymptotically stable. □

3. Dynamics analysis of the system with impulsive effect

According to Definition 2.1 in Chen et al. [5,34], system (1.4) constructs a semi-continuous dynamical system (Ω, f, φ, M), where $(x, y) \in \Omega \subset R_+^2$, $M = \{(x, y)|x = h\}$ is the impulse set. $f = f(p, t)$ is the semi-continuous dynamical system mapping with initial point $p = (x_0, y_0) \notin M$. The continuous function $\varphi : M \to N$ is called impulse mapping, $N = \{(x, y)|x = (1 - P_{\max}h/(h + \theta))\, h, 0 \le y \le \tau\}$ is the phase set. Obliviously $L : y = \frac{a-bx}{\beta(1+cx)}$ and Y-axis are two X-nullclines, and $L' : x = \frac{d}{\lambda\beta}$ and X-axis are two Y-nullclines. Next, we investigate the existence of order one period solution [5] by using method of successor functions [34], as well as the stability of periodic solutions by using Analogue of Poincaré Criterion [17] .

3.1. The existence of periodic solutions

According to the position of the impulse set and the phase set, we have the following theorems.

Theorem 3.1. *If $h \le \frac{d}{\lambda\beta}$, then system* (1.4) *has an order one periodic solution.*

Proof. For the case $h = \frac{d}{\lambda\beta}$, the impulse set and the Y-nullcline $x = \frac{d}{\lambda\beta}$ overlap. Let A (A_x, A_y) denote the intersection of N and L. We consider the orbit tangent to the point A, denoted as L_1. Assume L_1 intersects with M at point A_1, whose coordinate is denoted as $A_1(A_{1x}, A_{1y})$. Since $A_1 \in M$, the impulse set, then there exists $A_1^+ \in N$, such that $I(A_1) = A_1^+$, whose coordinate is denoted as $({A^+}_x, {A^+}_y)$, according to the definition of the successor function given in [34], if we denote the successor function as F, then we have $F(A) = {A_1^+}_y - A_y$. Consider the sign of ${A_1^+}_y - A_y$, there have three cases to be discussed.

Case a, ${A_1^+}_y - A_y = 0$, i,e., the point A and it's successor point A_1^+ overlap, obviously, according to the definition of the order one period solution given in [5], $\widehat{AA_1}$ constructs an order one periodic solution (see Figure 2(a)).

Case b, ${A_1^+}_y - A_y < 0$, i,e., the point A is above it's successor point A^+ (see Figure 2(b)). In this case, we have $F(A) < 0$. By Theorem 3.2 in [5], to prove the existence of periodic solution, we should find a point $P \in N$ such that $F(P) > 0$. For this purpose, we can choose a point $S \in N$ whose coordinate is denoted as (S_x, S_y). Consider the orbit pass by the point S, denoted as L_2. Let S_y is large enough, the L_2 can intersect with N twice. The second intersection with N is denoted as B, and the intersection of L_2 with the impulsive set M is denoted as B_1. Since $B_1 \in M$, the impulse set, then there exists $B_1^+ \in N$, such that $I(B_1) = B_1^+$, i.e., B_1^+ is the successor point of B. If the coordinate of B, B_1 and B_1^+ is denoted as and $(B_x, B_y), (B_{1x}, B_{1y})$ and $({B_1}^+{}_x, {B_1}^+{}_y)$ respectively, then we have $F(B) = {B_1^+}_y - B_y$. Because S_y is large enough, then B_y can be small enough such that $F(B) = {B_1^+}_y - B_y > 0$. Thus our aim has been achieved.

Case c, ${A_1^+}_y - A_y > 0$, i,e., the point A is below it's successor point A^+ (see Figure 2(c)). In this case, we have $F(A) > 0$. We consider the orbit L_2. Since S_y

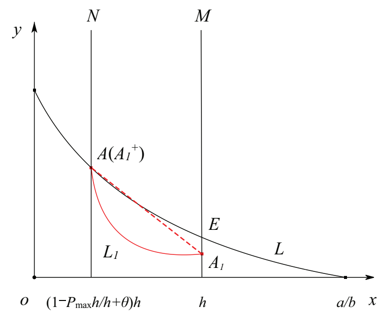

(a) Case a in Theorem 3.1.

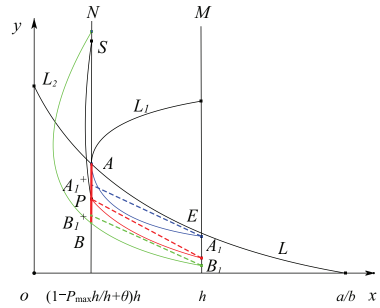

(b) Case b in Theorem 3.1.

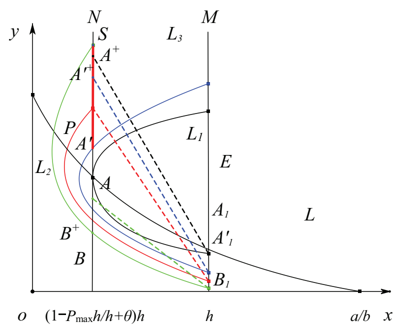

(c) Case c in Theorem 3.1.

Figure 2. Periodic solution for the case in Theorem 3.1

is large enough, then B_1 is below the point A_1, thus B_1^+ is also below the point A_1^+, this leads to $F(S) = {B_1^+}_y - S_y < 0$. Thus by Theorem 3.2 in [5], we know that system (1.3) produces an order one periodic solution.

For the case $h < \frac{d}{\lambda\beta}$, similar argument can continue, here we omit it.

This completes the proof. $\square$

Theorem 3.2. *If* $0 < (1 - P_{\max}h/(h+\theta))\,h < d/\lambda\beta < h < a/b$, *system* (1.3) *has an order one periodic solution.*

Proof. As discussed in Theorem 3.1, we should find two points point $P_1, P_2 \in N$ satisfying $F(Q_1)f(Q_2) < 0$. First, we claim that there must be a trajectory L_0 tangent to $x = h$ at point H. Let $\rho \geq 0$ represents the number of the intersections of trajectory L_0 and the phase set N. we have two cases to discuss.

Case a, if $0 \leq \rho \leq 1$, there exists a trajectory L_1 beginning from A and tangent to N at a point $A(A_x, A_y)$. The trajectory L_1 intersects with M at the point $A_1(A_{1x}, A_{1y})$. Since M is the impulse set, then there exists $A_1^+ \in N$, such that $\varphi(A_1) = A_1^+$, i.e., $A_1^+({A_1^+}_x, {A_1^+}_y)$ is the successor point of A. Then according to the position of A and A^+, we have two subcases here, (a1): ${A_1^+}_y - A_y \leq 0$ (please see Figure 3(a)), and (a2): ${A_1^+}_y - A_y > 0$ (see Figure 3(b)). Then as a similar discuss in the proof of Theorem 3.1, we can see system (1.4) has an order one periodic solution.

Case b, if $\rho = 2$, i.e., the trajectory L_0 intersect phase set twice, we denote the intersection point as A' and B', respectively. Denote the coordinate of A' and B'

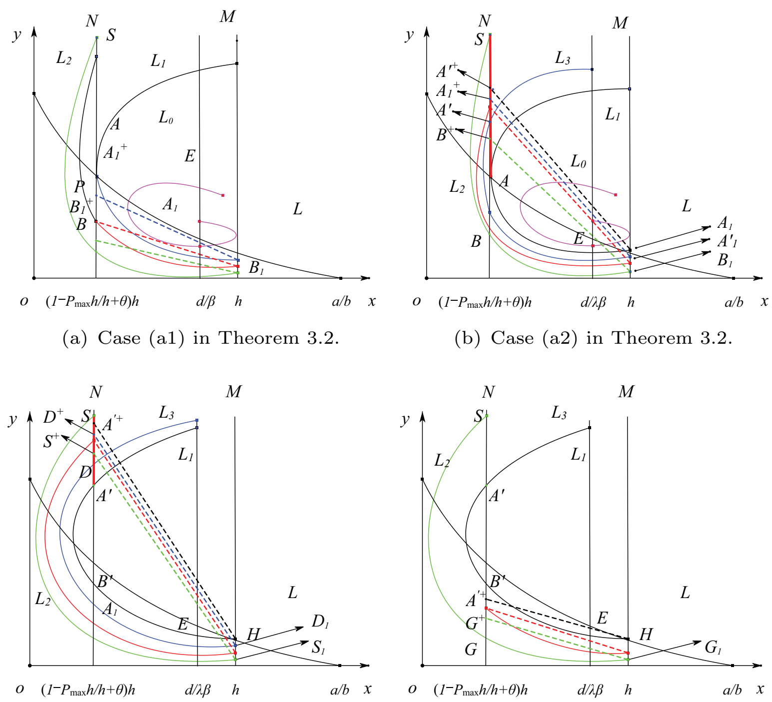

(a) Case (a1) in Theorem 3.2.

(b) Case (a2) in Theorem 3.2.

(c) Case (a3) in Theorem 3.2.

(d) Case (a4) in Theorem 3.2.

Figure 3. Periodic solution for the case in Theorem 3.2

as (A'_x, A'_y) and (B'_x, B'_y), respectively. Without loss of generality, we assume point A' is above point B', i.e., $A'_y > B'_y$. Since the trajectory L_0 tangent to the impulse set M at point H, then there exists $A'^+ \in N$, such that $I(H) = A'^+$, i.e., A'^+ is the successor point of A' or B'. According to the sign of $A'^+{}_y - A'_y$ and $A'^+{}_y - B'_y < 0$, we have two subcases to be discussed as well, case (b1) (please see Figure 3(c)) where $A^+_y - A_y > 0$ and (b2)(please see Figure 3(d)) where $A'^+{}_y - B'_y < 0$. As what we discussed in the proof of Theorem 3.1, we can also show that system (1.4) has an order one periodic solution. $\square$

Remark 3.1. If $\left(1 - \frac{P_{\max} h}{h+\theta}\right) h > \frac{d}{\lambda\beta}$, we can still prove the system (1.4) has an order one periodic solution. But in this case, under the control measures, the population of the pests keep a higher number($> \frac{d}{\lambda\beta}$), however, by the globally asymptotic stability of $E(x^*, y^*)$, such control measures do not have practical significance.

3.2. The stability of periodic solutions

Theorem 3.3. *Consider a periodic solution* $(x, y) = (\mu(t), \gamma(t))$ *of system* (1.4), *let* $\prod(A_0, t)$ *be the orbit beginning from* $A_0(\mu(0), \gamma(0))$, *where* $\mu(0) = \left(1 - P_{\max} \frac{h}{h+\theta}\right) h$, *then if*

$$\left| \frac{\frac{a - b\left(1 - P_{\max}\frac{h}{h+\theta}\right)h}{1 + c\left(1 - P_{\max}\frac{h}{h+\theta}\right)h} - \beta\gamma_0}{\frac{a - bh}{1 + ch} - \beta\frac{\gamma_0 - \tau}{1 - q}} \frac{\gamma_0 - \tau}{\gamma_0} \right| < 1,$$

then the periodic solution passing through point $(h, \gamma(T))$ *of system* (1.4) *is orbitally asymptotically stable.*

Proof. Consider an order one orbit starting from C_0, when the orbit touch to the impulse set (the intersection and the time are denoted by C_1 and T, respectively), a pulse happens at point C_1, the phase point is denoted by $C_1^+(\mu(T^+), \gamma(T^+))$. Then we obtain $C_1 = f(C_0, T), C_0 = C_1^+ = \varphi(C_1)$, and by the third and fourth equations of system (1.4), we have $\mu(T^+) = \left(1 - \frac{P_{\max} h}{h+\theta}\right)\mu(T) = \mu(0), \gamma(T^+) = (1-q)\gamma(T) + \tau = \gamma(0)$. Let

$$\begin{cases} \Gamma(x,y) = x(t)\frac{a-bx(t)}{1+cx(t)} - \beta x(t)y(t), \\ \Sigma(x,y) = y(\lambda\beta x - d), \\ \Theta_1(x,y) = -\frac{P_{\max} x}{x+\theta}x, \\ \Theta_2(x,y) = -qy + \tau, \\ \Phi(x,y) = x - h. \end{cases}$$

By a direct calculation, we get

$$\begin{cases} \frac{\partial\Theta_1}{\partial x} = -P_{\max}\frac{x(x+2\theta)}{(x+\theta)^2}, \\ \frac{\partial\Theta_1}{\partial y} = 0, \\ \frac{\partial\Theta_2}{\partial x} = 0, \\ \frac{\partial\Theta_2}{\partial y} = -q, \\ \frac{\partial\Phi}{\partial x} = 1, \\ \frac{\partial\Phi}{\partial y} = 0, \end{cases}$$

and

$$\begin{aligned} \int_0^T \frac{\partial\Gamma}{\partial x}dt &= \int_0^T \left(\frac{a-bx}{1+cx} - \beta y - \frac{(ac+b)x}{(1+cx)^2}\right)dt \\ &= \ln\left(\frac{\mu_1}{\mu_0}\right) - \int_0^T \frac{(ac+b)x}{(1+cx)^2}dt, \\ \int_0^T \frac{\partial\Sigma}{\partial y}dt &= \int_0^T (\lambda\beta x - d)dt \\ &= \ln\left(\frac{\gamma_1}{\gamma_0}\right). \end{aligned}$$

Then, we have

$$\begin{aligned} \Delta_1 &= \frac{\Gamma_+ \cdot \left(\frac{\partial\Theta_2}{\partial y}\frac{\partial\Phi}{\partial x} - \frac{\partial\Theta_2}{\partial x}\frac{\partial\Phi}{\partial y} + \frac{\partial\Phi}{\partial x}\right)}{\Gamma\cdot\left(\frac{\partial\Phi}{\partial x}\right) + \Sigma\cdot\left(\frac{\partial\Phi}{\partial y}\right)} \\ &\quad + \frac{\Sigma_+ \cdot \left(\frac{\partial\Theta_1}{\partial x}\frac{\partial\Phi}{\partial y} - \frac{\partial\Theta_1}{\partial y}\frac{\partial\Phi}{\partial x} + \frac{\partial\Phi}{\partial y}\right)}{\Gamma\cdot\left(\frac{\partial\Phi}{\partial x}\right) + \Sigma\cdot\left(\frac{\partial\Phi}{\partial y}\right)} \\ &= \frac{\Gamma(\mu(T^+), \gamma(T^+))(1-q)}{\Gamma(\mu(T), \gamma(T))} \end{aligned}$$

$$
\begin{aligned}
&= \frac{\Sigma(\mu_0,\gamma_0)(1-q)}{\Gamma(\mu(T),\gamma(T))} \\
&= \frac{\left(1-P_{\max}\frac{h}{h+\theta}\right) h \left(\frac{a-b\left(1-P_{\max}\frac{h}{h+\theta}\right)h}{1+c\left(1-P_{\max}\frac{h}{h+\theta}\right)h} - \beta\gamma_0\right)(1-q)}{h\left(\frac{a-bh}{1+ch} - \beta\frac{\gamma_0-\tau}{1-q}\right)} \\
&= \frac{\left(1-P_{\max}\frac{h}{h+\theta}\right) \left(\frac{a-b\left(1-P_{\max}\frac{h}{h+\theta}\right)h}{1+c\left(1-P_{\max}\frac{h}{h+\theta}\right)h} - \beta\gamma_0\right)(1-q)}{\frac{a-bh}{1+ch} - \beta\frac{\gamma_0-\tau}{1-q}}.
\end{aligned}
$$

Thus,

$$
\begin{aligned}
\omega_2 &= \Delta_1 \exp\left\{\int_0^T \left(\frac{\partial \Gamma}{\partial x} + \frac{\partial \Sigma}{\partial y}\right) dt\right\} \\
&= \frac{\left(1-P_{\max}\frac{h}{h+\theta}\right) \left(\frac{a-b\left(1-P_{\max}\frac{h}{h+\theta}\right)h}{1+c\left(1-P_{\max}\frac{h}{h+\theta}\right)h} - \beta\gamma_0\right)(1-q)}{\frac{a-bh}{1+ch} - \beta\frac{\gamma_0-\tau}{1-q}} \\
&\quad \exp\left\{\ln\left(\frac{\mu_1}{\mu_0}\right) + \ln\left(\frac{\gamma_1}{\gamma_0}\right) - \int_0^T \frac{(ac+b)x}{(1+cx)^2} dt\right\} \\
&= \frac{\left(1-P_{\max}\frac{h}{h+\theta}\right) \left(\frac{a-b\left(1-P_{\max}\frac{h}{h+\theta}\right)h}{1+c\left(1-P_{\max}\frac{h}{h+\theta}\right)h} - \beta\gamma_0\right)(1-q)}{\frac{a-bh}{1+ch} - \beta\frac{\gamma_0-\tau}{1-q}} \\
&\quad \frac{\mu_1}{\mu_0}\frac{\gamma_1}{\gamma_0} \exp\left\{-\int_0^T \frac{(ac+b)x}{(1+cx)^2} dt\right\} \\
&= \frac{\left(1-P_{\max}\frac{h}{h+\theta}\right) \left(\frac{a-b\left(1-P_{\max}\frac{h}{h+\theta}\right)h}{1+c\left(1-P_{\max}\frac{h}{h+\theta}\right)h} - \beta\gamma_0\right)(1-q)}{\frac{a-bh}{1+ch} - \beta\frac{\gamma_0-\tau}{1-q}} \\
&\quad \frac{h}{\left(1-P_{\max}\frac{h}{h+\theta}\right)h} \frac{\frac{\gamma_0-\tau}{1-q}}{\gamma_0} \exp\left\{-\int_0^T \frac{(ac+b)x}{(1+cx)^2} dt\right\} \\
&= \frac{\frac{a-b\left(1-P_{\max}\frac{h}{h+\theta}\right)h}{1+c\left(1-P_{\max}\frac{h}{h+\theta}\right)h} - \beta\gamma_0}{\frac{a-bh}{1+ch} - \beta\frac{\gamma_0-\tau}{1-q}} \frac{\gamma_0-\tau}{\gamma_0} \exp\left\{-\int_0^T \frac{(ac+b)x}{(1+cx)^2} dt\right\} \\
&< \frac{\frac{a-b\left(1-P_{\max}\frac{h}{h+\theta}\right)h}{1+c\left(1-P_{\max}\frac{h}{h+\theta}\right)h} - \beta\gamma_0}{\frac{a-bh}{1+ch} - \beta\frac{\gamma_0-\tau}{1-q}} \frac{\gamma_0-\tau}{\gamma_0}.
\end{aligned}
$$

Hence, by Analogue of Poincaré Criterion [17], the periodic solution is orbitally asymptotically stable if

$$
\left|\frac{\frac{a-b\left(1-P_{\max}\frac{h}{h+\theta}\right)h}{1+c\left(1-P_{\max}\frac{h}{h+\theta}\right)h} - \beta\gamma_0}{\frac{a-bh}{1+ch} - \beta\frac{\gamma_0-\tau}{1-q}} \frac{\gamma_0-\tau}{\gamma_0}\right| < 1.
$$

This completes the proof . □

4. Numerical simulations

In this section, to verify the existence of periodic solution of the model, we will give some numerical simulations. We set the basic parameters as $a = 1, b = 1, c = 1, \beta = 0.5, \lambda = 1.6, P_{\max} = 0.9, \theta = 0.2, q = 0.4$, and get the system as follows,

$$\begin{cases} \left.\begin{aligned} x'(t) &= x(t)\tfrac{1-x(t)}{1+x(t)} - 0.5x(t)y(t), \\ y'(t) &= 0.8x(t)y(t) - 0.4y(t), \end{aligned}\right\} x \neq h, \\ \left.\begin{aligned} \Delta x(t) &= -\tfrac{0.9x(t)}{x(t)+0.2}x(t), \\ \Delta y(t) &= -0.4y(t) + \tau, \end{aligned}\right\} x = h. \end{cases} \tag{4.1}$$

For the system neglecting impulsive effect, by simple calculations, we get the positive equilibrium $E^*(0.5, 0.667)$. The direction field shows that system has a stable focus, please see Figure 4. It can be seen from Figure 4 that the number of pests and natural enemies is finally stable at $E^*(0.5, 0.667)$.

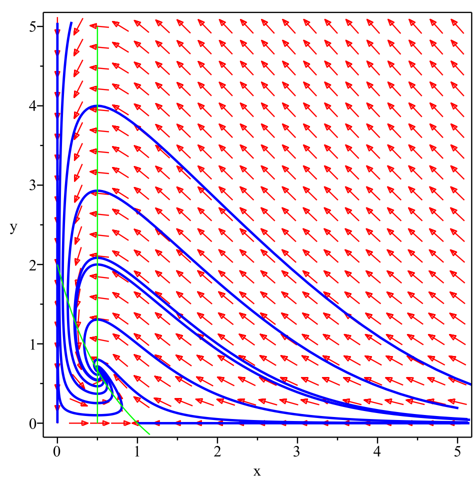

Figure 4. System (4.1) has a stable focus.

Let the initial value be $(0.2, 0.2)$, following the theoretical results, we have the following cases.

Case I: Let $h = 0.5$, by adjusting the release amount of natural enemies, there will be two sub-cases.

Case I(a): Supplementing (releasing) a larger number of natural enemies (for example $\tau = 0.2$), It can be seen from the red curve in Figure 5(b) and Figure 5(c) respectively, that the number of natural enemies oscillates from 0.15 to 0.342 and the number of pests oscillates from 0.1786 to 0.5. Moreover, this oscillation is periodic, Figure 5(a) shows that system (4.1) produces an order one periodic solution, see the red curve in Figure 5(a).

Case I(b): Supplementing (releasing) a small number of natural enemies (for example $\tau = 0.1$), which allows the number of natural enemies to return to a lower level under the effect of the pulse, as shown in the green curve in Figure 5(c), the number of natural enemies oscillate from 0.15 to 0.342. Due to the effect of the pulse, the number of pests oscillates from 0.1786 to 0.5 periodically as shown in the green curve in Figure 5(b). The green curve in Figure 5(a) shows that system (4.1) produces an order one periodic solution.

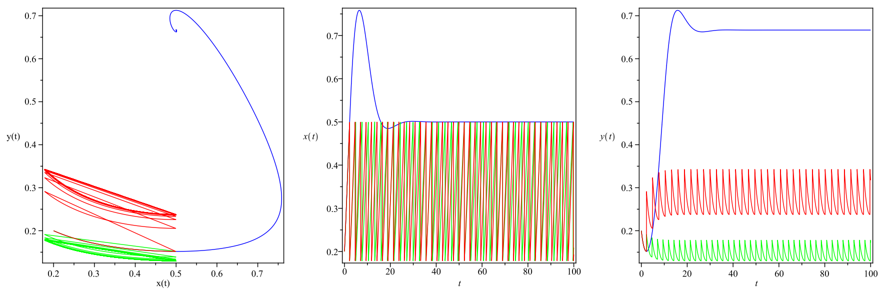

(a) Phase diagram of $x(t)$ and $y(t)$. (b) Time series of $x(t)$. (c) Time series of $y(t)$.

Figure 5. Compare of solutions of the system with impulsive effect (red or green curve) and without impulsive effect(blue curve), where $h = 0.5$.

Case II: Take a tighter control strategy, for example let $h = 0.4 < 0.5$, according to different release amount of natural enemies, we find that the number of natural enemies oscillate from 0.15 to 0.35 for the case $\tau = 0.1$ (see the green curve in Figure 6(c)) and from 0.15 to 0.35 for the case $\tau = 0.2$ (see the red curve in Figure 6(c)). And the number of pests oscillates from 0.16 to 0.4 periodically (see Figure 6(b)), moreover, system (4.1) produces an order one periodic solution, see Figure 5(a), the red curve is for the case $\tau = 0.2$ and the green curve is for the case $\tau = 0.1$.

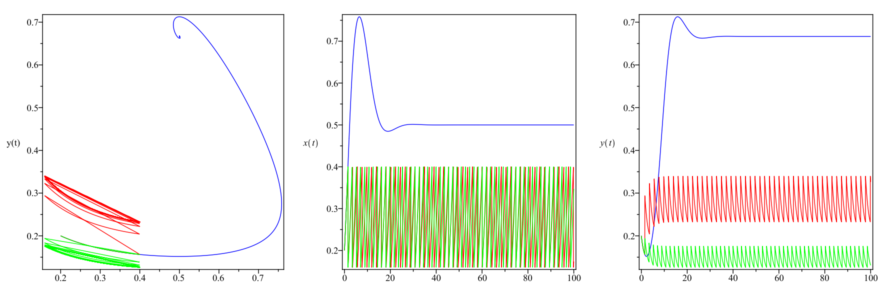

(a) Phase diagram of $x(t)$ and $y(t)$. (b) Time series of $x(t)$. (c) Time series of $y(t)$.

Figure 6. Compare of solutions of the system with impulsive effect (red or green curve) and without impulsive effect(blue curve), where $h = 0.4$.

Case III: Take a looser control strategy, for example let $h = 0.7$. By regulating τ, we find that pests and natural enemies produce periodic changes in the system (4.1) , see Figure 7(b) and Figure 7(c) respectively, the red curve is for the case of $\tau = 0.2$ and the red curve is for the case of $\tau = 0.1$. The number of pests ranges from 0.21 to 0.7. Moreover, we can clearly see from Figure 7(a) that system (4.1) produces one order one periodic solution with $\tau = 0.2$ (the red orbit in Figure 7(a)) and $\tau = 0.1$ (the green orbit in Figure 7(a)), respectively.

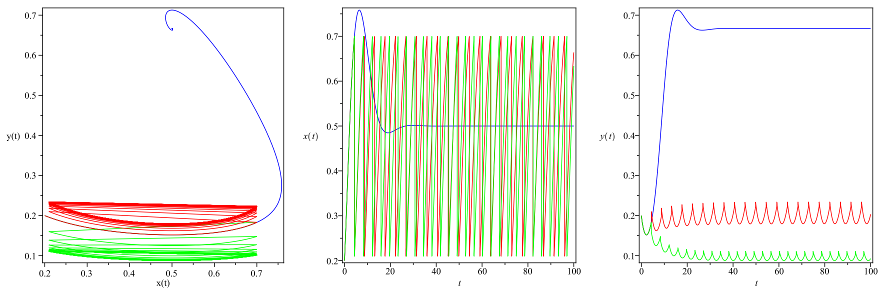

(a) Phase diagram of $x(t)$ and $y(t)$. (b) Time series of $x(t)$. (c) Time series of $y(t)$.

Figure 7. Compare of solutions of the system with impulsive effect (red or green curve) and without impulsive effect(blue curve), where $h = 0.7$.

Table 1. The periodic solution of system (4.1) with different parameters

Impulse set	Phase set	μ	The corresponding Figure
$x = 0.5$	0.1786	0.2	red curve in Figure 5(a)
$x = 0.5$	0.1786	0.1	green curve in Figure 5(a)
$x = 0.4$	0.16	0.2	red curve in Figure 6(a)
$x = 0.4$	0.16	0.1	green curve in Figure 6(a)
$x = 0.7$	0.21	0.2	red curve in Figure 7(a)
$x = 0.7$	0.21	0.1	green curve in Figure 7(a)

5. Conclusion

In present paper, a nonlinear impulsive state feedback control system was establish to model the integrated pest control in a food-limited environments. Impulsive state feedback control is properly used to describe the change of the number of pests and natural enemies reduced by human intervention activities in a pest management. Mathematically, a simple and intuitive geometric analysis is used to indicate the existence of periodic solutions. The results of the paper show impulsive state feedback control plays a good role in the integrated pest management, the pests have not been eradicated, but been suppressed below the economic threshold level, this implies we can reduce the usage of pesticide to control the pests.

Acknowledgements. The authors are grateful to the anonymous referees for their useful suggestions which improve the contents of this article.

References

[1] J. L. Apple and R. F. Smith (Eds), *Integrated pest management*, Springer, Boston, 1976.

[2] D. Atwood and C. Paisley-Jones, *Pesticides Industry Sales and Usage 2008-2012 Market Estimates*, Tech. rep., U.S. Environmental Protection Agency, Washington, DC., 2017.

[3] D. Auslander, *Spatial effects on the stability of a food-limited moth population*, J. Franklin Inst., 1982, 314(6), 347–365.

[4] J. Chen, T. Zhang, Z. Zhang et al., *Stability and output feedback control for singular markovian jump delayed systems*, Math. Control Relat. Fields, 2018, 8(2), 475–490.

[5] L. Chen, X. Liang and Y. Pei, *The periodic solutions of the impulsive state feedback dynamical system*, Commun. Math. Biol. Neurosci., 2018, 2018, Article ID 14.

[6] M. Chi and W. Zhao, *Dynamical analysis of multi-nutrient and single microorganism chemostat model in a polluted environment*, Adv. Difference Equ., 2018, 2018(1), 120.

[7] M. Chi and W. Zhao, *Dynamical analysis of two-microorganism and single nutrient stochastic chemostat model with monod-haldane response function*, Complexity, 2019, 2019, Article ID 8719067, 13 pages.

[8] X. Fan, Y. Song and W. Zhao, *Modeling cell-to-cell spread of HIV-1 with nonlocal infections*, Complexity, 2018, 2018, Article ID 2139290, 10 pages.

[9] J. Gao, B. Shen, E. Feng and Z. Xiu, *Modelling and optimal control for an impulsive dynamical system in microbial fed-batch culture*, Comp. Appl. Math., 2013, 32(2), 275–290.

[10] N. Gao, Y. Song, X. Wang and J. Liu, *Dynamics of a stochastic sis epidemic model with nonlinear incidence rates*, Adv. Difference Equ., 2019, 2019(1), 41.

[11] H. Guo and L. Chen, *Periodic solution of a turbidostat system with impulsive state feedback control*, J. Math. Chem., 2009, 46(4), 1074–1086.

[12] M. Hernández and A. Margalida, *Pesticide abuse in europe: effects on the cinereous vulture (aegypius monachus) population in spain*, Ecotoxicology, 2008, 17(4), 264–272.

[13] S. B. Hsu, *Ordinary Differential Equations with Applications*, World Scientific, Singapore, 1999.

[14] G. Jiang, Q. Lu and L. Qian, *Complex dynamics of a holling type II prey-predator system with state feedback control*, Chaos Solitons Fractals, 2007, 31(2), 448–461.

[15] Z. Jiang, X. Bi, T. Zhang and B. S. A. Pradeep, *Global hopf bifurcation of a delayed phytoplankton–zooplankton system considering toxin producing effect and delay dependent coefficient*, Math. Biosci. Eng., 2019, 16(5), 3807–3829.

[16] Z. Jiang, W. Zhang, J. Zhang and T. Zhang, *Dynamical analysis of a phytoplankton–zooplankton system with harvesting term and holling iii functional response*, Internat. J. Bifur. Chaos Appl. Sci. Engrg., 2018, 28(13), 1850162.

[17] V. Lakshmikantham, D. D. Bainov and P. S. Simeonov, *Theory of Impulsive Differential Equations*, World Scientific, Singapore, 1989.

[18] G. Li and M. Chen, *Infinite horizon linear quadratic optimal control for stochastic difference time-delay systems*, Adv. Difference Equ., 2015, 2015(1), 14.

[19] Y. Li, H. Cheng and Y. Wang, *A lycaon pictus impulsive state feedback control model with allee effect and continuous time delay*, Adv. Difference Equ., 2018, 2018(1), 367.

[20] Y. Li, Y. Li, Y. Liu and H. Cheng, *Stability analysis and control optimization of a prey-predator model with linear feedback control*, Discrete Dyn. Nat. Soc., 2018, 2018, Article ID 4945728, 12 pages.

[21] Z. Li, L. Chen and J. Huang, *Permanence and periodicity of a delayed ratio-dependent predator-prey model with holling type functional response and stage structure*, J. Comput. Appl. Math., 2009, 233(2), 173–187.

[22] J. Liang, S. Tang, R. A. Cheke and J. Wu, *Adaptive release of natural enemies in a pest-natural enemy system with pesticide resistance*, Bull. Math. Biol., 2013, 75(11), 2167–2195.

[23] B. Liu, Y. Zhang and L. Chen, *The dynamical behaviors of a Lotka-Volterra predator-prey model concerning integrated pest management*, Nonlinear Anal. Real World Appl., 2005, 6(2), 227–243.

[24] F. Liu and H. Wu, *A note on the endpoint regularity of the discrete maximal operator*, Proc. Amer. Math. Soc., 2019, 147(2), 583–596.

[25] G. Liu, Z. Chang and X. Meng, *Asymptotic analysis of impulsive dispersal predator-prey systems with markov switching on finite-state space*, J. Funct. Spaces, 2019, 2019, Article ID 8057153, 18 pages.

[26] G. Liu, X. Wang, X. Meng and S. Gao, *Extinction and persistence in mean of a novel delay impulsive stochastic infected predator-prey system with jumps*, Complexity, 2017, 2017, Article ID 1950970, 15 pages.

[27] H. Liu and H. Cheng, *Dynamic analysis of a prey–predator model with state-dependent control strategy and square root response function*, Adv. Difference Equ., 2018, 2018(1), 63.

[28] K. Liu, T. Zhang and L. Chen, *State-dependent pulse vaccination and therapeutic strategy in an SI epidemic model with nonlinear incidence rate*, Comput. Math. Methods Med., 2019, 2019, Article ID 3859815, 10 pages.

[29] X. Liu, Y. Li and W. Zhang, *Stochastic linear quadratic optimal control with constraint for discrete-time systems*, Appl. Math. Comput., 2014, 228, 264–270.

[30] T. Ma, X. Meng and Z. Chang, *Dynamics and optimal harvesting control for a stochastic one-predator-two-prey time delay system with jumps*, Complexity, 2019, 2019, Article ID 5342031, 19 pages.

[31] X. Meng and L. Zhang, *Evolutionary dynamics in a Lotka-Volterra competition model with impulsive periodic disturbance*, Math. Methods Appl. Sci., 2016, 39(2), 177–188.

[32] X. Meng, S. Zhao and W. Zhang, *Adaptive dynamics analysis of a predator-prey model with selective disturbance*, Appl. Math. Comput., 2015, 266, 946–958.

[33] A. Miao, T. Zhang, J. Zhang and C. Wang, *Dynamics of a stochastic SIR model with both horizontal and vertical transmission*, J. Appl. Anal. Comput., 2018, 8(4), 1108–1121.

[34] G. Pang and L. Chen, *Periodic solution of the system with impulsive state feedback control*, Nonlinear Dynam., 2014, 78(1), 743–753.

[35] Z. Shi, J. Wang, Q. Li and H. Cheng, *Control optimization and homoclinic bifurcation of a prey–predator model with ratio-dependent*, Adv. Difference Equ., 2019, 2019(1), 2.

[36] F. E. Smith, *Population dynamics in daphnia magna and a new model for population growth*, Ecology, 1963, 44(4), 651–663.

[37] R. F. Smith and H. T. Reynolds, *Principles, definitions and scope of integrated pest control*, in *Proceedings of the FAO symposium on Integrated pest control*, 1965.

[38] Y. Song, A. Miao, T. Zhang et al., *Extinction and persistence of a stochastic SIRS epidemic model with saturated incidence rate and transfer from infectious to susceptible*, Adv. Difference Equ., 2018, 2018(1), 293.

[39] K. Sun, T. Zhang and Y. Tian, *Dynamics analysis and control optimization of a pest management predator-prey model with an integrated control strategy*, Appl. Math. Comput., 2017, 292, 253–271.

[40] S. Tang, Y. Xiao, L. Chen and R. A. Cheke, *Integrated pest management models and their dynamical behaviour*, Bull. Math. Biol., 2005, 67(1), 115–135.

[41] Y. Tian, K. Sun and L. Chen, *Modelling and qualitative analysis of a predator-prey system with state-dependent impulsive effects*, Math. Comput. Simulation, 2011, 82(2), 318–331.

[42] G. Wang and S. Tang, *Qualitative analysis of prey-predator model with non-linear impulsive effects*, Appl. Math. Mech.-Engl. Ed., 2013, 34(5), 496–505.

[43] J. Wang, H. Cheng, Y. Li and X. Zhang, *The geometrical analysis of a predator-prey model with multi-state dependent impulsive*, J. Appl. Anal. Comput., 2018, 8(2), 427–442.

[44] J. Wang, K. Liang, X. Huang et al., *Dissipative fault-tolerant control for non-linear singular perturbed systems with markov jumping parameters based on slow state feedback*, Appl. Math. Comput., 2018, 328, 247–262.

[45] M. E. Whalon, D. Mota-Sanchez and R. M. Hollingworth, *Global Pesticide Resistance in Arthropods*, Commonwealth Agricultural Bureaux International, Cambridge, 2008.

[46] C. Yin, Y. Cheng, S.-M. Zhong and Z. Bai, *Fractional-order switching type control law design for adaptive sliding mode technique of 3d fractional-order nonlinear systems*, Complexity, 2015, 21(6), 363–373.

[47] S. Yuan, P. Li and Y. Song, *Delay induced oscillations in a turbidostat with feedback control*, J. Math. Chem., 2011, 49(8), 1646–1666.

[48] J. Zhang, J. Xia, W. Sun et al., *Finite-time tracking control for stochastic nonlinear systems with full state constraints*, Appl. Math. Comput., 2018, 338, 207–220.

[49] S. Zhang, X. Meng, T. Feng and T. Zhang, *Dynamics analysis and numerical simulations of a stochastic non-autonomous predator-prey system with impulsive effects*, Nonlinear Anal. Hybrid Syst., 2017, 26, 19–37.

[50] T. Zhang, X. Liu, X. Meng and T. Zhang, *Spatio-temporal dynamics near the steady state of a planktonic system*, Comput. Math. Appl., 2018, 75(12), 4490–4504.

[51] T. Zhang, W. Ma, X. Meng and T. Zhang, *Periodic solution of a prey-predator model with nonlinear state feedback control*, Appl. Math. Comput., 2015, 266, 95–107.

[52] T. Zhang, X. Meng, Y. Song and T. Zhang, *A stage-structured predator-prey SI model with disease in the prey and impulsive effects*, Math. Model. Anal., 2013, 18(4), 505–528.

[53] L. Zhao, L. Chen and Q. Zhang, *The geometrical analysis of a predator-prey model with two state impulses*, Math. Biosci., 2012, 238(2), 55–64.

[54] W. Zhao, J. Liu, M. Chi and F. Bian, *Dynamics analysis of stochastic epidemic models with standard incidence*, Adv. Difference Equ., 2019, 2019(1), 22.

[55] Z. Zhao, T. Wang and L. Chen, *Dynamic analysis of a turbidostat model with the feedback control*, Commun. Nonlinear Sci. Numer. Simul., 2010, 15(4), 1028–1035.

[56] F. Zhu, X. Meng and T. Zhang, *Optimal harvesting of a competitive n-species stochastic model with delayed diffusions*, Math. Biosci. Eng., 2019, 16, 1554–1574.

[57] X. Zhuo, *Global attractability and permanence for a new stage-structured delay impulsive ecosystem*, J. Appl. Anal. Comput., 2018, 8(2), 457–457.

[58] X.-L. Zhuo and F.-X. Zhang, *Stability for a new discrete ratio-dependent predator–prey system*, Qual. Theory Dyn. Syst., 2018, 17(1), 189–202.